

## Quantum Light Emission of Two Lateral Tunnel-Coupled (In, Ga)As/GaAs Quantum Dots Controlled by a Tunable Static Electric Field

G. J. Beirne,<sup>1</sup> C. Hermannstädter,<sup>1</sup> L. Wang,<sup>2</sup> A. Rastelli,<sup>2</sup> O. G. Schmidt,<sup>2</sup> and P. Michler<sup>1</sup>

<sup>1</sup>*Physikalisches Institut, Universität Stuttgart, Pfaffenwaldring 57, 70569 Stuttgart, Germany*

<sup>2</sup>*Max-Planck-Institut für Festkörperforschung, Heisenbergstr. 1, 70569 Stuttgart, Germany*

(Received 9 September 2005; published 4 April 2006)

Lateral quantum coupling between two self-assembled (In,Ga)As quantum dots has been observed. Photon statistics measurements between the various excitonic and biexcitonic transitions of these lateral quantum dot molecules display strong antibunching confirming the presence of coupling. Furthermore, we observe an anomalous exciton Stark shift with respect to static electric field. A simple model indicates that the lateral coupling is due to electron tunneling between the dots when the ground states are in resonance. The electron probability can then be shifted to either dot and the system can be used to create a wavelength-tunable single-photon emitter by simply applying a voltage.

DOI: [10.1103/PhysRevLett.96.137401](https://doi.org/10.1103/PhysRevLett.96.137401)

PACS numbers: 78.67.Hc, 73.21.La, 78.55.Cr

Future progress in experimental quantum computation and quantum cryptography using solids relies on the ability to produce both compact and reliable quantum gates, and new types of nonclassical light sources, e.g., tunable single-photon sources. To date, the use of single semiconductor quantum dots (QDs) together with significant progress in QD optics has led to the demonstration of fundamental new devices [1], such as single-photon sources [2–4], an optically controlled electron spin memory device [5], an optically triggered single-electron turnstile [6], and an all optical quantum gate [7].

An essential element for further progress and subsequent new functionalities is the introduction of a controllable quantum coupling between two or more QDs; e.g., different schemes already exist for scalable quantum computing based on coupled QDs [8–10]. Furthermore, coupled QDs have been proposed as a possible entangled photon source [11]. Thus, an electrically tunable lateral QD molecule (QDM) could potentially be used as the basic building block of a quantum computer (quantum gate) and could also allow for the voltage-controlled emission of nonclassical light.

To date, coupled QDs have been fabricated by both cleaved edge overgrowth [12] and self-assembled growth techniques [13]. Quantum coupling in individual QDMs and its manipulation using static electric fields ( $E$  fields) has also been demonstrated [14,15]. In each of these experiments the QDs were vertically coupled along the growth direction, i.e., in one dimension. For applications, however, one would normally prefer to laterally couple QDs because, in principle, the lateral geometry enables coupling in two dimensions, and thus allows for a natural up-scaling to very large numbers of quantum gates across a semiconductor substrate. Furthermore, for individual lateral QDMs the realization of reliable gating between the constituent QDs should be relatively straightforward when compared to the vertical QDM case, where gating, although feasible, is technically very demanding. More-

over, the lateral positioning of QDs and QDMs has already been demonstrated [16,17].

In this work, lateral quantum coupling has been observed between two (In, Ga)As/GaAs QDs and the degree of coupling has been estimated from the anomalous exciton Stark shift as a function of static  $E$  field. In addition, we have found that the single-photon emission from the QDM can be switched between two wavelengths simply by applying a voltage.

The self-assembled lateral QDMs were produced on GaAs(001) substrates by a unique combination of molecular beam epitaxy and *in situ* atomic layer precise etching [16–18] which provides a low density ( $5 \times 10^7 \text{ cm}^{-2}$ ) homogeneous ensemble of QDMs consisting of two dots aligned along the  $[1\bar{1}0]$  direction (see Fig. 1). The QDM photoluminescence (PL) emission energy was blueshifted to 1.32 eV, by interrupting the growth of the capping layer for 4 min following the deposition of 2 nm of GaAs. This enabled the detection of QDM PL using Si-based detectors. The QDMs were then capped by a 100 nm GaAs layer to improve the optical quality.

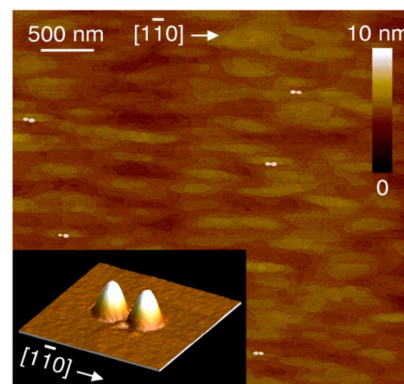


FIG. 1 (color online). Atomic force microscope image of the lateral (In, Ga)As/GaAs QDMs. The inset ( $200 \times 200 \text{ nm}^2$ ) clearly shows that each QDM consists of two QDs.

Micro-PL and photon statistics measurements were performed on single QDMs at 4 K. A tunable Ti:sapphire laser (700–1000 nm) was used and could be operated in either continuous wave (cw) or pulsed mode (2 ps wide pulses at 76.2 MHz). When recording spectra, the PL was dispersed using a 0.75 m spectrometer and detected using a liquid-nitrogen-cooled charge coupled device. For the photon correlation measurements the PL lines were spectrally selected using two monochromators, one in each arm of a Hanbury-Brown and Twiss type setup [19], and detected using two avalanche photodiodes.

We have studied 15 QDMs to date and two typical cw PL spectra recorded at low excitation power density (PD) from single QDMs (molecule *A* and *B*) are presented in Figs. 2(a) and 2(b). Two intense, sharp lines (*X1* and *X2*) separated by an energy of between 0.5 and 1.7 meV (depending on the QDM) dominate the spectra, and two less intense lines, *Y* and *Z*, are also invariably present at an energy of approximately  $4.5 \pm 1.5$  meV and  $5.5 \pm 1.5$  meV below the *X2* peak, respectively. In Figs. 2(c) and 2(d) two additional PL lines (*XX1* and *XX2*) emerge at higher PDs and are typically located 1.0 to 2.5 meV below the corresponding *X1* and *X2* peaks, in line with the usual Coulomb binding energy of biexcitons in (In, Ga)As/GaAs QDs. The 6 observed PL lines are not linearly polarized.

As shown in Figs. 2(e) and 2(f), the *X1*, *X2*, *Y*, and *Z* peaks show a linear increase of their integrated PL intensity with PD; a dependence consistent with the behavior of excitons. We therefore propose that the *X1* and *X2* lines are due to neutral exciton recombination in the QDM. In con-

trast, the two peaks *XX1* and *XX2* which appear at higher PDs display a superlinear dependence as expected for biexcitons. Such observations demonstrate that the QDM is composed of two distinct QDs, even though the QDs are separated by only a few nanometers of barrier material.

The high PD spectrum of molecule *A* also displays two peaks on the low energy side of the *Z* line. Because of a lack of signal we are unable to identify these features; however, they may originate from the extra pair of biexciton transitions expected from a QDM, i.e., the case where one hole is confined in each dot [20]. Also, we do not observe indirect exciton transitions, resulting from the recombination of an electron in one dot and a hole in the other, as the large center-to-center distance combined with the relatively large (8 nm average) interdot barrier strongly suppresses hole tunneling and thus the indirect electron-hole wave function overlap is negligible.

The nature of the *Y* and *Z* lines is not clear at present, however, these peaks may originate from charged exciton transitions in the QDM. A number of observations point to this possibility: (1) both are visible at low PDs, (2) the integrated PL intensities of both display a linear power dependence, (3) an unequal number of electrons and holes is quite probable in nonresonantly pumped QDs, (4) the cross-correlation between *Y* (*Z*) and *X1* or *X2* exhibits antibunching, and (5) no bunching is observed in the latter cross-correlations implying that *Y* and *Z* are not part of a cascaded emission process [21].

Second order cross-correlation function [ $g^{(2)}(\tau)$ ] measurements between the PL lines of molecule *B* have been performed in order to verify the presence of quantum coupling between the dots and also to further examine the nature of these lines. In these experiments, if the two dots are independent of each other we expect  $g^{(2)}(\tau)$  to equal one for all  $\tau$  [20]. In other words, if an independent QD emits a photon, nothing prevents a neighboring QD from emitting a photon simultaneously; therefore, antibunching will not be observed at  $\tau = 0$ . In contrast, however, we have observed pronounced antibunching in the cross-correlations between *X1* and *X2* [Fig. 3(a)]; this clearly demonstrates the presence of coupling in the QDM.

In Fig. 3(b), an antibunching dip rapidly followed by a bunching peak [21] is observed in the cross-correlation between *X1* and *XX1* (also observed between *X2* and *XX2*, not shown). This implies that the *XX1* (*XX2*) line not only originates from the QDM but also forms a radiative cascade with the *X1* (*X2*) transition. In Figs. 3(c) [3(d)] the result of the cross-correlation carried out between *Y* (*Z*) and *X2* is presented. A clear antibunching dip is apparent at  $\tau = 0$ , therefore the QDM is also the source of the *Y* (*Z*) line.

Figure 3(e) presents the results of a pulsed autocorrelation measurement performed on the *X2* line from another QDM. A strong suppression of coincidence events is observed at  $\tau = 0$ . The Poisson-normalized levels given in the figure were calculated from the coincidence data and

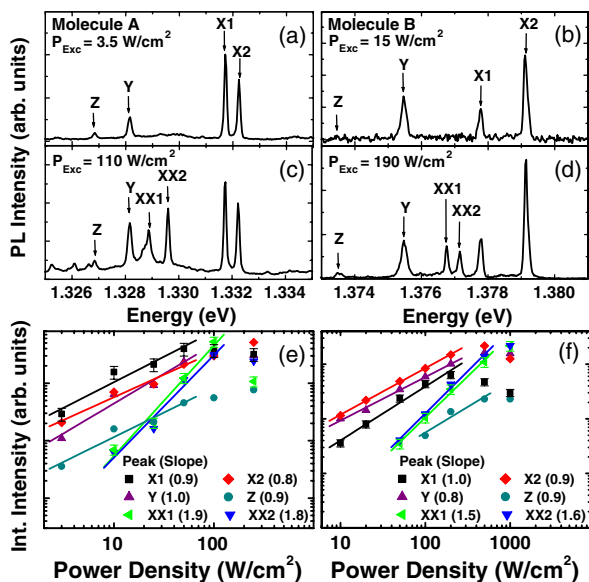


FIG. 2 (color online). PL spectra recorded at 4 K from two single QDMs (molecule *A* and *B*) under nonresonant cw excitation (800 nm, 1.55 eV) at low PD [(a) and (b), 4 peaks] and at high PD [(c) and (d), 6 peaks]. In (e) and (f) the integrated PL intensity of the peaks is plotted as a function of PD with excitons and biexcitons exhibiting a typical linear (slope  $\approx 1$ ) and superlinear dependence (slope  $\approx 1.7$ ), respectively.

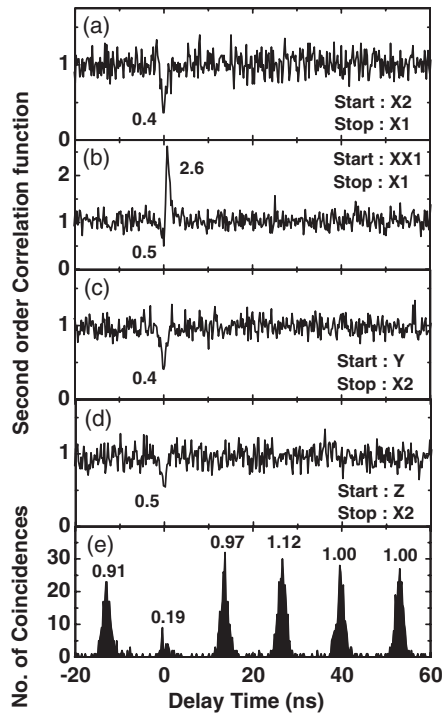


FIG. 3. Second order cross-correlation measurements from molecule *B* at 4 K using 800 nm (1.55 eV) cw excitation and a PD of 300 W/cm<sup>2</sup>, between (a) X2 and X1, (b) X1 and the associated biexciton (XX1), (c) Y and X2, and (d) Z and X2.  $g^{(2)}(\tau)$  at  $\tau = 0$  is given for each [ $g^{(2)}(\tau) < 1.0$  ( $> 1$ ) indicates antibunching (bunching)]. (e) Autocorrelation of X2, using pulsed excitation at 800 nm and a PD of 750 W/cm<sup>2</sup>.

the value of 0.19 obtained for  $g^{(2)}(\tau)$  at  $\tau = 0$  indicates a factor of  $\sim 5$  decrease in multiphoton emission pulses compared to a Poissonian source of the same average intensity.

So far, we have verified the presence of quantum coupling in the QDMs and have also shown that they can be used to generate nonclassical light. We now demonstrate, using electrical contacts processed on the sample surface, that the coupling can be controlled by applying an  $E$  field along the QDM axis. The  $E$  field was applied using interdigital gate electrodes with 30  $\mu\text{m}$  wide Schottky contacts separated by 15  $\mu\text{m}$ . Typical QDM PL spectra recorded as a function of  $E$  field are displayed in Fig. 4(a). At  $-2.0$  V, the X2 line dominates the spectrum, and is observed to redshift slightly with decreasing negative voltage. For smaller negative fields ( $-1.0$  V) the X1 line starts to emerge until at  $-0.35$  V (the alignment bias) both lines possess approximately the same intensity. For positive voltages (1.0 V) the X2 peak effectively vanishes and the X1 peak dominates. This characteristic anticorrelated behavior of the X1 and X2 relative intensities has been observed from several QDMs and clearly points to the influence of quantum coupling in the system. In contrast, when the  $E$  field is turned by 90° and is applied perpendicular to the QDM axis, no such switching behavior is observed, thus eliminating the possibility that all 6 peaks

originate from a single QD, which should exhibit a similar behavior for both field orientations.

The X1 and X2 peak emission energies are plotted as a function of  $E$  field in Fig. 4(b) and the field-dependent shift of each is found to consist of both linear and quadratic contributions. At a bias of 1.0 V, both lines exhibit the minimum emission energy over the investigated range. As the bias is reduced, X1 and X2 exhibit a blue Stark shift; however, at values close to the alignment bias ( $-0.35$  V), we observe an anomalous redshift with respect to the interpolated peak energy expected from the shift on both the higher and the lower voltage side of each [dashed curves in Fig. 4(b)]. A similar anomalous Stark shift has been reported for vertically coupled QDs and is considered to provide strong evidence for the presence of quantum coupling between QDs [22]. This redshift is interpreted as a resonance between the electron ground states of the QDs and reflects the influence of tunneling processes that result in a redistribution of the electron wave function across both dots. This implies that we only observe exciton transitions associated with the electron symmetric state in PL spectra. The reason for the absence of excitons associated with the electron antisymmetric state is not clear; however, this may

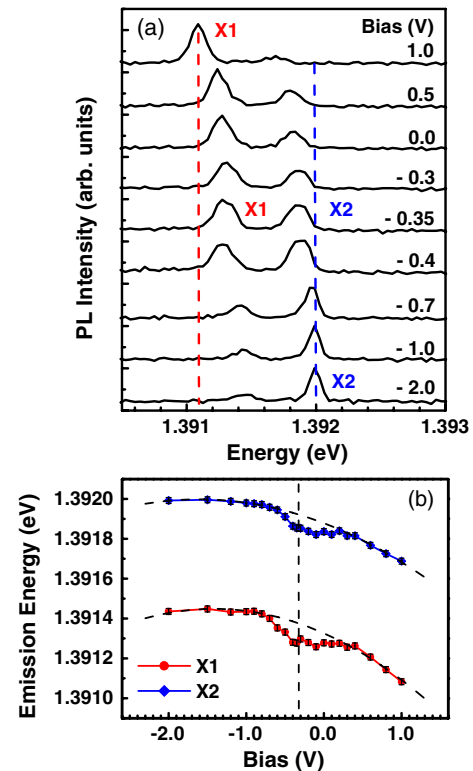


FIG. 4 (color online). (a) QDM PL spectra at 4 K, and (b) the PL peak energy of X1 and X2 as a function of applied voltage along the QDM axis under pulsed excitation at 818 nm (1.52 eV) and a PD of 200 W/cm<sup>2</sup>. A redshift is apparent at the alignment bias (dashed vertical line) indicating that the electron ground states of the two QDs are in resonance. The dashed curves are guides to the eye indicating the expected behavior without coupling.



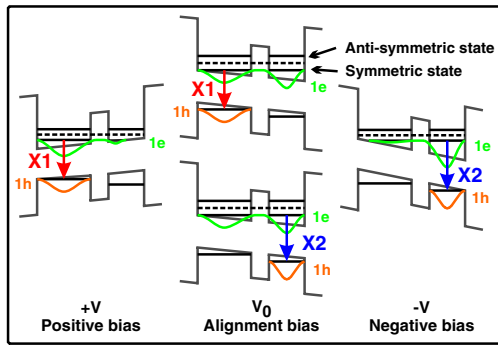


FIG. 5 (color online). Schematic diagrams illustrating the predictions of the 1D model used to qualitatively describe the coupling mechanism and its control using an  $E$  field.

be due to the transitions being partly dark. If we now consider that the tunnel coupling energy  $\Delta$  of slightly different, adjacent QDs manifests itself as a redshift of  $\Delta/2$  at the anticrossing, we can use the anomalous Stark shift, which averages  $90 \mu\text{eV}$ , to estimate a lateral coupling energy of  $180 \pm 15 \mu\text{eV}$ .

Quantum coupling between QDs can occur either by electron/hole tunneling or via Coulomb interaction (Förster transfer) [23,24]. At relatively large interdot separations Coulomb coupling is more probable than single-particle tunneling and the exciton states are made up of localized single-particle states, however, at nanoscale separations electron tunneling becomes increasingly probable and the exciton states can then consist of delocalized electron states. Clearly, a full configuration model, such as that presented by Bester *et al.*, is necessary for a detailed understanding of such coupling mechanisms [25]. Although such a model is beyond the scope of this work, we have employed a 1D model to qualitatively understand and illustrate the processes at work in a QDM at various  $E$  fields. The results are schematically presented in Fig. 5. We have assumed that the dots are separated by an  $8 \pm 4$  nm barrier with a reduced bandgap and that the smaller and larger QD in the QDM has a diameter of 34 and 36 nm, respectively, (35 nm average diameter, see Fig. 1). The confined single-particle 1D electron and hole wave functions were then calculated numerically by solving the Schrödinger equation.

The model predicts that holes remain localized in the QDs, while electrons become almost entirely delocalized at the alignment bias, forming symmetric and antisymmetric states across the QDM. This result is in agreement with electron and hole tunneling rates predicted by more sophisticated models [25] and results from the different effective mass of electrons and holes in the interdot GaAs barrier material, i.e., 0.067 and 0.48 that of the free electron mass, respectively. The model estimates an electron coupling energy (electron ground state energy splitting) of 20 and  $500 \mu\text{eV}$  for an interdot barrier width of 12 and 4 nm, respectively. In addition, the experimental estimate of  $180 \pm 15 \mu\text{eV}$  indicates that the effective barrier

width in the investigated QDM is between 6 and 7 nm. When applying more positive or negative  $E$  fields the model also predicts the observed switching behavior, i.e., the electronic ground state wave function can be transferred to either the larger or the smaller dot, enhancing the X1 or the X2 transition, respectively. Hence, the optical transition rate of X1 or X2 can effectively be switched on or off, allowing for the deterministic emission of single photons [see Fig. 3(e)] at either the X1 or the X2 emission energy. Future measurements will aim to directly control the tunnel barrier in a QDM by placing a gate electrode between the two QDs, and also to scale up to QDMs containing three or more QDs [16–18].

In conclusion, we have fabricated pairs of laterally coupled (In,Ga)As QDs and demonstrated interdot electron coupling using optical techniques. The degree of tunnel coupling can be controlled by applying a static  $E$  field along the QDM axis and a coupling energy of  $180 \pm 15 \mu\text{eV}$  has been estimated from the anomalous Stark shift of the QDM neutral excitons. Finally, by applying a voltage we have also shown that the electron probability can be reversibly shifted to either QD and that the QDM can be used to create a wavelength-tunable single-photon emitter.

The authors acknowledge financial support from the Alexander von Humboldt Foundation, the Deutsche Forschungsgemeinschaft (SFB/TR21), and the Bundesministerium für Bildung und Forschung (03N8711).

- 
- [1] A. Badolato *et al.*, *Science* **308**, 1158 (2005).
  - [2] P. Michler *et al.*, *Science* **290**, 2282 (2000).
  - [3] C. Santori *et al.*, *Nature (London)* **419**, 594 (2002).
  - [4] Z. Yuan *et al.*, *Science* **295**, 102 (2002).
  - [5] M. Kroutvar *et al.*, *Nature (London)* **432**, 81 (2004).
  - [6] A. Zrenner *et al.*, *Nature (London)* **418**, 612 (2002).
  - [7] X. Li *et al.*, *Science* **301**, 809 (2003).
  - [8] E. Biolatti *et al.*, *Phys. Rev. Lett.* **85**, 5647 (2000).
  - [9] X.-Q. Li and Y. Arakawa, *Phys. Rev. A* **63**, 012302 (2000).
  - [10] B. W. Lovett *et al.*, *Phys. Rev. B* **68**, 205319 (2003).
  - [11] O. Gywat, G. Burkard, and D. Loss, *Phys. Rev. B* **65**, 205329 (2002).
  - [12] G. Schedelbeck *et al.*, *Science* **278**, 1792 (1997).
  - [13] M. Bayer *et al.*, *Science* **291**, 451 (2001).
  - [14] H.J. Krenner *et al.*, *Phys. Rev. Lett.* **94**, 057402 (2005).
  - [15] G. Ortner *et al.*, *Phys. Rev. Lett.* **94**, 157401 (2005).
  - [16] O.G. Schmidt *et al.*, *IEEE J. Sel. Top. Quantum Electron.* **8**, 1025 (2002).
  - [17] R. Songmuang, S. Kiravittaya, and O.G. Schmidt, *Appl. Phys. Lett.* **82**, 2892 (2003).
  - [18] B. Krause *et al.*, *Phys. Rev. B* **72**, 085339 (2005).
  - [19] S.M. Ulrich *et al.*, *Appl. Phys. Lett.* **83**, 1848 (2003).
  - [20] B.D. Gerardot *et al.*, *Phys. Rev. Lett.* **95**, 137403 (2005).
  - [21] E. Moreau *et al.*, *Phys. Rev. Lett.* **87**, 183601 (2001).
  - [22] R. Oulton *et al.*, *Physica (Amsterdam)* **26E**, 302 (2005).
  - [23] A.O. Govorov, *Phys. Rev. B* **71**, 155323 (2005).
  - [24] A. Nazir *et al.*, *Phys. Rev. B* **71**, 045334 (2005).
  - [25] G. Bester, A. Zunger, and J. Shumway, *Phys. Rev. B* **71**, 075325 (2005).